UNIVERSITETET I TRONDHEIM
NORGES TEKNISKE HØGSKOLE
INSTITUTT FOR FYSIKK

Faglig kontakt under eksamen:
Navn: Eivind H. Hauge
Tlf.: 3651

EKSAMEN I FAG 74944 - TRANSPORTTEORI 2
Fredag 20. mai 1994
Tid: kl. 0900-1400

Tillatte hjelpemidler: K. Rottmann: Mathematische Formelsammlung
S. Barrett og T.M. Cronin: Mathematical Formulae
Godkjent lommekalkulator

NB!
1. Tabell over naturkonstanter er gitt på side 4.
2. Alle underpunkt i oppgavesettet har i utgangspunktet lik vekt.
3. Vær oppmerksom på at et punkt ofte kan besvares uavhengig av tidligere punkt i oppgaven.

Oppgave 1

I denne oppgaven skal vi diskutere enkle modeller for en "kvanteledning" (quantum wire) i en 2-dimensjonal elektrongass (2DEG) i xy-planet, påtrykt et perpendikulært magnetfelt, $\vec{B} = B\hat{z}$. Kvanteledninger som dette vil vanligvis være definert ved et ytre elektrostatisk potensial, V(y). Siden systemet, pr. antakelse, er translasjonsinvariant i x-retningen, kan vi skrive bølgefunksjonen på formen $\psi(x,y) = e^{ikx}\phi_k(y)$.

a Velg gauge $\vec{A} = (A_x,0,0)$ og vis at Schrödingerlikningen med konstant B-felt og den antatte løsningsform lyder

$$\left[-\frac{\hbar^2\partial^2}{2m\partial y^2} + \frac{1}{2}m\omega_c^2 (y-kl_B^2)^2 + V(y) \right]\phi_k(y) = \varepsilon_k\phi_k(y)$$

der m er den effektive masse, $\omega_c = eB/m$ er syklotronfrekvensen og $l_B = \sqrt{\hbar/eB}$ den magnetiske lengden.

b Se først på det enkleste spesialtilfellet, $V(y) \equiv 0$, og bestem energispektret (Landau-nivåene), $\varepsilon_{k,n}$, ved analogibetraktning til et velkjent problem. Hva er gruppehastigheten

$$v_n = \frac{1}{\hbar} \frac{\partial \varepsilon_{k,n}}{\partial k}$$

for bevegelse i x-retning i dette tilfellet?

Vi tar nå for oss den typiske situasjon at magnetfeltet er sterkt, og det ytre potensialet langsomt varierende, i betydningen

$$\frac{\partial V}{\partial y} \cdot l_B \ll \hbar\omega_c \quad ; \quad \frac{\partial^2 V}{\partial y^2} l_B^2 \ll \hbar\omega_c$$

Bølgefunksjonene $\psi_{k,n} = e^{ikx}\phi_{k,n}(y)$ vil da være lokalisert i en stripe rundt $y = kl_B^2$, med bredde av størrelsesorden l_B. Med $\eta \equiv y - kl_B^2$ kan vi derfor, til ledende orden, nøye oss med å bruke et tilnærmet uttrykk for $V(y)$:

$$V(y) = V(kl_B^2) + V'(kl_B^2) \cdot (y - kl_B^2)$$

$$\equiv \frac{1}{2} m\omega_c^2 (\nu_k + \nu_k' \eta)$$

c Vis at Schrödingerlikningen under disse betingelsene kan skrives som

$$\{-\frac{\hbar^2}{2m} \frac{\partial^2}{\partial \eta^2} + \frac{1}{2} m\omega_c^2 [(\eta + \frac{1}{2}\nu_k')^2 + \nu_k - \frac{1}{4}(\nu_k')^2]\} \phi_k(\eta) = \varepsilon_k \phi_k(\eta)$$

Også denne gang kan energispektret finnes ved analogibetraktninger. Gjør dette, og vis at gruppehastigheten til ledende orden stemmer overens med det klassiske uttrykket

$$\vec{v}_{drift} = (\vec{E} \times \vec{B})/B^2$$

der $\vec{E} = -\nabla V/e$ er det elektriske feltet.

d La nå det elektrostatiske potensialet være null, $V(y) = 0$, men la B-feltet, $\vec{B} = B(y)\hat{z}$, være langsomt varierende som funksjon av y, $B(y) = B_0 + B_1 y$. Det kan vises (du skal ikke vise dette) at resultatet er en drift i x-retning gitt som

$$v_n \simeq \frac{\hbar B_1}{m|B_0|}(n + \frac{1}{2})$$

Forsøk å sannsynliggjøre dette resultatet, så langt det er mulig, ved å skissere klassiske elektronbaner for dette tilfellet.

e Vi antar at den 2-dimensjonale elektrongassen befinner seg i GaAs. Gjør et klassisk (numerisk) overslag over hvor stor den elektriske feltstyrken må være i pkt. c for at den kinetiske energien knyttet til driftbevegelsen, E_{drift}, er 1% av splittingen, $\hbar\omega_c$, mellom Landaunivåene ved B = 1T.

Gjør dessuten et overslag, på basis av formelen oppgitt i pkt. d, over $E_{drift}/\hbar\omega_c$ når driften skyldes gradienter i et makroskopisk generert B-felt på 1T, romlig konsentrert innen lineære dimensjoner av størrelsesorden 1 cm.

Kommentarer?

Oppgave 2

Vedlagt finner du kopi av deler (Abstract, Sec. II og delvis Sec. III) av en nylig publisert artikkel av en japansk-tysk gruppe, med von Klitzing som sentral forfatter. Les først gjennom det kopierte materialet for å få et overblikk over hva det dreier seg om, uten forsøk på å få med deg alle detaljer. Ta deretter for deg spørsmålene nedenfor, som henviser til spesielle deler av materialet.

Merk: De kraftig opptrukne linjene i Fig. 1a, b representerer (ioneimplanterte) fikserte negative ladningslinjer, som virker som frastøtende "vegger" for de mobile elektronene i den 2-dimensjonale elektrongassen (2DEG). Interessen fokuseres på elektrontransport i parallelledningene definert ved disse "veggene", og koplet ved "vinduet" vist i Fig. 1b.

a Påstand midt i høyre spalte, Sec. II: "..... Fermi energy [---] given by $E_F = (h^2/4\pi m^*)n$ for a 2D electron-gas at low temperature,...". Vis at denne påstanden følger av at tilstandstettheten ved B = 0 er $\rho(E) = g_s g_v(m^*/2\pi\hbar^2)$.

b Fig. 2 og 3 viser at for to forskjellige prøver, med henholdsvis W = 1.25 μm og W = 0.65 μm, er Hall-motstanden, R_H, ca. 13 kΩ for $B > B_c \approx 3.5$T. Hvilken konklusjon kan trekkes av at $R_H \approx 13$ kΩ? Hvorfor er verdien av B_c omtrent den samme for de to prøvene? (Merk at Fermienergien er omtrent den samme).

c Tilbake til midt i høyre spalte, Sec: II: "The carrier density (n), determined from Shubnikov-De Haas (SdH) oscillations in a high magnetic-field region, ...". Forklar kort den fysiske bakgrunnen for utsagnet.

d Første avsnitt, Sec. III: "At B = 0T, R_{L1} becomes negative [---], and this negative resistance disappears with increasing magnetic field". Gi en kvalitativ forklaring på dette (setningen etter den siterte gir et hint).

e Fig. 3 (den lille prøven) viser noenlunde periodiske oscillasjoner, spesielt i R_{L1}, i området B ~ 3.5T. Perioden er, som en ser, ca. 50 mT. Kan du foreslå en forklaring på dette?

[f Har du tid og lyst, er det fritt fram for flere kommentarer og delforklaringer knyttet til artikkelen].

CONSTANTS AND CONVERSION FACTORS
(to four significant figures)

speed of light	$c = 2.998 \times 10^8$ m/s
electron charge unit	$e = 1.602 \times 10^{-19}$ C
Coulomb force constant	$\frac{1}{4\pi\varepsilon_0} = 8.988 \times 10^9$ N · m^2/C^2
	$\frac{e^2}{4\pi\varepsilon_0} = 1.440$ eV · nm
electron mass	$m_e = 9.109 \times 10^{-31}$ kg $= 0.5110$ MeV/c^2
proton mass	$M_p = 1.673 \times 10^{-27}$ kg $= 938.3$ MeV/c^2
proton–electron mass ratio	$\frac{M_p}{m_e} = 1836$
Planck's constant	$h = 6.626 \times 10^{-34}$ J · s $= 4.136 \times 10^{-15}$ eV · s
	$hc = 1240$ eV · nm
	$\hbar = 1.055 \times 10^{-34}$ J · s $= 6.582 \times 10^{-16}$ eV · s
	$\hbar c = 197.3$ eV · nm
Avogadro's number	$N_A = 6.022 \times 10^{23}$ mole^{-1}
Boltzmann's constant	$k_B = 1.381 \times 10^{-23}$ J/K $= 8.617 \times 10^{-5}$ eV/K
electron Compton wavelength	$\frac{h}{m_e c} = 2.426 \times 10^{-12}$ m
Bohr radius	$a_0 = 5.292 \times 10^{-11}$ m
Rydberg energy unit	$E_0 = 13.61$ eV
Rydberg constant	$R_\infty = 1.097 \times 10^7$ m^{-1}
fine structure constant	$\alpha = \frac{1}{137.0}$
Bohr magneton	$\mu_B = 9.274 \times 10^{-24}$ A · m^2 $= 5.788 \times 10^{-9}$ eV/G
nuclear magneton	$\mu_N = 3.152 \times 10^{-12}$ eV/G
gravitational constant	$G = 6.673 \times 10^{-11}$ N · m^2/kg^2
electron volt	eV $= 1.602 \times 10^{-19}$ J
atomic mass unit	u $= 1.661 \times 10^{-27}$ kg $= 931.5$ MeV/c^2
cross section unit	barn $= 10^{-28}$ m^2 $= (10$ fm$)^2$
light-year	lt-y $= 9.461 \times 10^{15}$ m

Effective mass in GaAs

$m^* = 0.067\, m_e$

Side 5 av 8

PHYSICAL REVIEW B VOLUME 48, NUMBER 11 15 SEPTEMBER 1993-I

Transport characteristics of a window-coupled in-plane-gated wire system

Y. Hirayama and Y. Tokura
NTT Basic Research Laboratory, Musashino-Shi, Tokyo 180, Japan

A. D. Wieck, S. Koch,* R. J. Haug, and K. von Klitzing
Max-Planck-Institut für Festkörperforschung, Heisenbergstrasse 1, W-7000 Stuttgart 80, Germany

K. Ploog
Paul-Drude-Institut für Festkörperelektronik, Hausvogteiplatz 5-7, O-1086 Berlin, Germany
(Received 13 April 1993)

Low-temperature ($T \approx 50$ mK) transport characteristics are measured for parallel wires coupled by a ballistic window. The structure is fabricated by focused Ga ion-beam scanning and subsequent annealing. The size of the structure is modified by in-plane-gated operation. At zero magnetic field, the transport characteristics are governed by the mode matching between one-dimensional modes in the wires and quasi-zero-dimensional modes in the window. When four-terminal resistance is measured as a function of in-plane-gate voltage, a small period oscillation is superimposed on the background oscillation corresponding to the subband population in each wire. At intermediate magnetic fields, Aharonov-Bohm interference effects are observed in both the magnetic field and the in-plane-gate voltage dependence. These originate from the circulating channel in the window. Theoretical calculations essentially reproduce the experimental results, supporting these explanations.

by considering the simple models. These experimental and theoretical results are discussed in this paper.

II. FABRICATION AND MEASUREMENTS

The parallel in-plane-gated (IPG) wires coupled by a small window were formed on an $Al_xGa_{1-x}As$-GaAs modulation-doped heterostructure by focused Ga ion-beam (Ga-FIB) scanning. The initial two-dimensional (2D) electron gas had a carrier density n of 1.6×10^{11} cm^{-2} and a mobility of μ of 5×10^5 $cm^2/V\,s$ at 1.5 K before illumination. A schematic structure of the system is shown in Fig. 1(a), and the central region of the system is enlarged in Fig. 1(b). The Ga-FIB with an acceleration energy of 100 kV and a beam diameter of about $\phi=100$ nm was scanned along the thick solid lines. The interval between the centers of parallel implanted lines is denoted by W, and the length of the unimplanted space along the center line by L. The ion dose was about 10^{12} cm^{-2} and subsequent annealing was carried out at 730 °C to remove implantation-induced damage. Highly resistive regions formed in the Ga-FIB scanned regions remained even after annealing, and depletion spreading from the Ga-FIB scanned lines defined the 2D electron gas.[20] Finally, Au/Ge/Ni ohmic contacts (labeled 1–6) were formed to each 2D electron gas region. Narrow parallel wires were defined between 1 and 2 and between 3 and 4, and they were coupled by a small window at the center. A gate voltage applied to 5 and 6 modulated the depletion region spreading (W_{dep2}) through a lateral field effect (in-plane-gate operation).[21] Thus the effective wire width (W_{eff}) and vertical width of the window ($W_{wind}=2W-2W_{dep2}=2W_{eff}+2W_{dep1}$) could be controlled by gate voltages V_{g5} and V_{g6}. We fabricated two types of structures: a large one with $W=1.25$ μm and $L=1.2$ μm, and a small one with $W=0.65$ μm and $L=0.6$ μm.

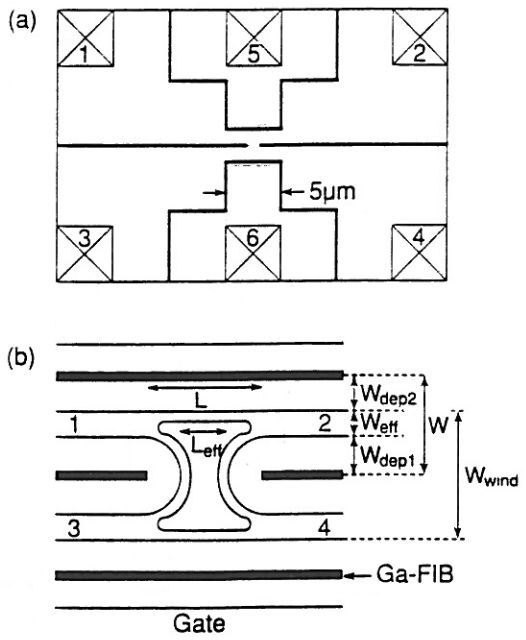

FIG. 1. A schematic diagram of parallel wires coupled by a ballistic window (a). The center region surrounded by the dotted lines is magnified in (b). Black lines indicate Ga-FIB-scanned lines, and ohmic contacts to the 2DEG are indicated by boxed X's and labeled by 1–6. Shadowed regions in (b) represent the depletion region spreading from Ga-implanted lines. In-plane gates (5 and 6) are used to modulate W_{dep2}, and consequently W_{eff}.

Transport characteristics were measured at a lattice temperature of about 50 mK using a dilution refrigerator. The actual electronic temperature might have been somewhat higher due to heating effects, but these would not influence the conclusions of the present work. Three kinds of four-terminal resistance $R_{L1}=R_{12,34}=(V_3-V_4)/I_{1-2}$, $R_{L2}=R_{42,31}$, and $R_H=R_{32,41}$ were measured as a function of magnetic field and in-plane-gate voltage. Here, the same voltage was applied both to 5 and 6 ($V_g=V_{g5}=V_{g6}$). A lock-in technique with a constant ac current of 10 nA was used in this measurement. Reducing the ac current level to 1 nA slightly changed the characteristics in the high-magnetic-field region ($B>5$ T), but not in the low-field region, which includes the complicated fine interference structures. Moreover, the carrier density was gradually increased by repeating a brief illumination at low temperature. The carrier density (n), determined from Shubnikov-De Haas (SdH) oscillations in a high-magnetic-field region, and Fermi energy (E_F) have a simple relation given by $E_F=(h^2/4\pi m^*)n$ for a 2D electron-gas approximation at low temperature, so we indicate E_F in the figures. The depletion spreading decreased with E_F (or carrier density). It was about 500 nm at $E_F=6$ meV ($n=1.8\times10^{11}$ cm^{-2}) and about 250 nm at $E_F=7.7$ meV ($n=2.3\times10^{11}$ cm^{-2}).[19,22] Therefore, the effective wire width W_{eff} of terminal wires was about 250 nm for the large structure when $E_F=6$ meV. For the small system, we need a larger E_F to open the terminal wires. $W_{eff}\approx150$ nm was obtained at $E_F=7.7$ meV. We measured the characteristics when more than five subbands were occupied in each wire, because symmetric ($R_{12,12}\sim R_{34,34}$) and stable characteristics cannot be obtained for a very small wire width. the horizontal window width L_{eff} was estimated from $L-2(W_{dep1}-\phi/2)$, where ϕ is the FIB diameter. Furthermore, the spreading of the depletion region at the edge of Ga-scanned line may be slightly smaller than $W_{dep1}-\phi/2$ due to a reduction in ion dose at the edge. Therefore, $L_{eff}>W_{eff}$ at $V_g=0$ V for both the small and large structures.

III. MAGNETOTRANSPORT CHARACTERISTICS

Transport characteristics were measured as a function of magnetic field at about 50 mK for both the large and small structures. Typical results are shown in Fig. 2 for the large structure, and in Fig. 3 for the small one. The in-plane-gate voltage $V_g=V_{g5}=V_{g6}$ was kept at $V_g=0$ V for both figures. At $B=0$ T, R_{L1} becomes negative, as already observed at 1.5 K, and this negative resistance disappears with increasing magnetic field. This behavior is explained by a sideways ballistic coupling between 1 and 4 (or 2 and 3).[19] This negative resistance is more enhanced for the large structure than for the small one.

Side 7 av 8

Furthermore, fine structures appear at 50 mK, unlike the 1.5-K measurements. The R_{L1} curve in Fig. 2 indicates fine structures in a low-magnetic-field region. Although a variation in background resistance in a low-field region obscures such fine structures in the R_{L2} and R_H curves, these curves contain similarities, as shown below. These fine structures are more enhanced in the small structure, as shown in Fig. 3. Here, the fine structures are clear in every curve (R_{L1}, R_{L2}, and R_H). This is due both to the small window size and the small effective wire width for the small structure under the experimental conditions. In the R_{L1} and R_{L2} curves of Fig. 3, a slowly varying background oscillation, probably corresponding to the SdH oscillations, is visible down to a low magnetic field, and their peak positions agree with the subband depopulation characteristics of each wire.[19] It is noteworthy that fine structures also appear in the quantum Hall regime in Fig. 3. A clear oscillation appears in both R_{L1} and R_{L2} at the higher-field side of the peak between $i=2$ and 4, where i is the filling factor. These oscillations are discussed later in connection with the AB-type interference effects.

Magnetoresistance characteristics in a low-magnetic-field region were studied in detail, and results are shown in Figs. 4 and 5. The in-plane-gate voltage was kept at $V_g=0$ V for these figures. Figure 4 shows characteristics for the large structure, and Fig. 5 for the small structure. Many periodic and aperiodic fine structures appear as a function of magnetic field, and they are completely reproducible as long as the sample is kept at a low temperature. We also measured the characteristics when V_g and/or E_F were varied. The amplitude of fine structures

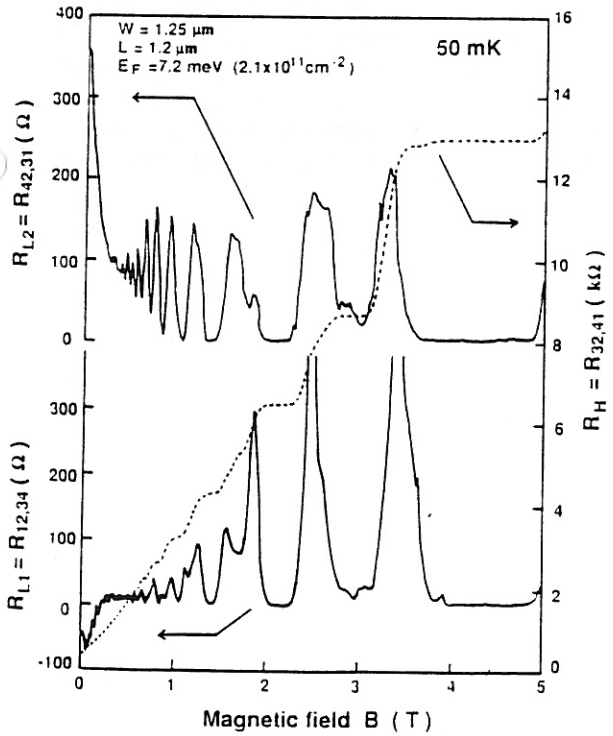

FIG. 2. Four-terminal resistances of the large devices ($W=1.25$ μm and $L=1.2$ μm) measured as a function of magnetic field at 50 mK. $E_F=7.2$ meV and $V_g=0$ V. This condition approximately corresponds to $W_{\text{eff}}\approx 600$ nm. R_{L1}, R_{L2}, and R_H, respectively, correspond to $R_{12,34}$, $R_{42,31}$, and $R_{32,41}$.

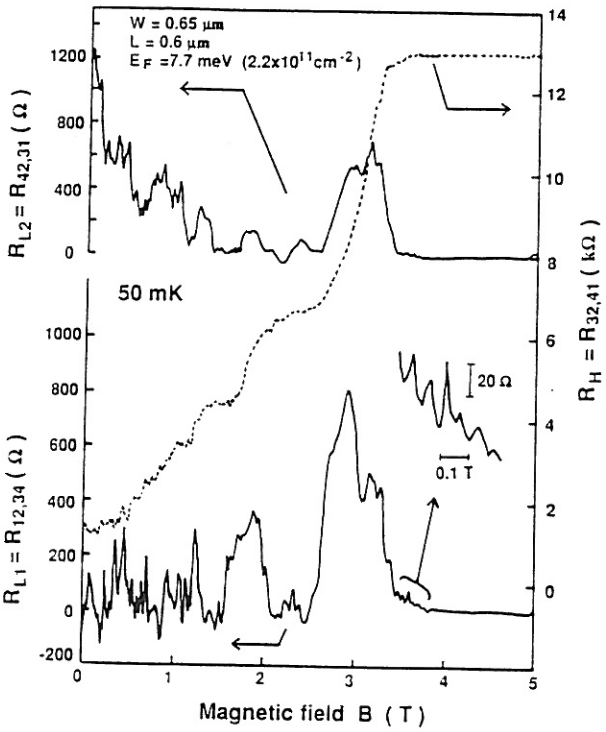

FIG. 3. Four-terminal resistances of the small devices ($W=0.65$ μm and $L=0.6$ μm) measured as a function of magnetic field at 50 mK. $E_F=7.7$ meV and $V_g=0$ V. This condition approximately corresponds to $W_{\text{eff}}\approx 150$ nm.

decreases with E_F (in other words, carrier density) and V_g. This suggests that a narrower W_{eff} is important to obtain distinct fine patterns. In addition, the oscillation period has a tendency to decrease as E_F and V_g increase.

Other interesting features in Fig. 4 are that the oscilla-

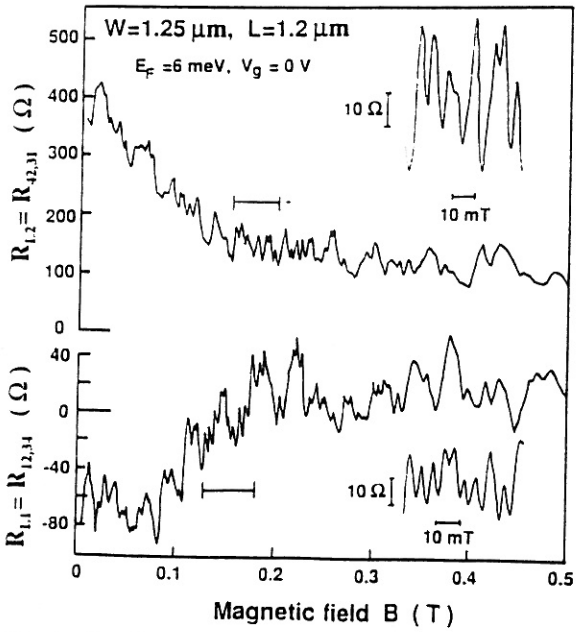

FIG. 4. Detailed traces of $R_{L1}=R_{12,34}$ and $R_{L2}=R_{42,31}$ for the large device measured at 50 mK in a low-magnetic-field region. $E_F=6$ meV and $V_g=0$ V. This value approximately corresponds to $W_{\text{eff}}\approx 250$ nm. Insets show enlarged signals in the field regions indicated by horizontal bars. The slowly varying background is subtracted in these insets.

Side 8 av 8

tion period varies as a function of magnetic field, and that it has a minimum at around $B=0.2$ T, where both the negative R_{L1} and the drastic decrease in R_{L2} disappear. Oscillations in this magnetic-field range are shown enlarged in the insets of Fig. 4. The slowly varying background is subtracted, so that fine oscillation patterns become clear in these insets. The average period is $\Delta B \sim 6$ mT at $E_F=6$ meV. Although the oscillation is less regular with large than with small E_F, the average period decreases with E_F and becomes $\Delta B \sim 4$ mT at $E_F=7.6$ meV. The peak interval increases in the lower-field region. The average period around $B=0$ T is about twice that around $B=0.2$ T. The peak interval also increases in the larger field region ($B \gtrsim 0.3$ T), and fine structures finally disappear leaving SdH oscillation. These characteristics of fine structure are similar in both R_{L1} and R_{L2}. However, the amplitude of fine oscillations is twice as large in R_{L2} than in R_{L1}.

Similar characteristics are reproduced for the small structure (see Fig. 5), except that peak intervals become large and the oscillation amplitude is enhanced. Although the small interval structures are seen in some parts of the R_{L2} curve, the most regular and smallest interval of about $\Delta B=20$ mT is observed at around $B=0.6$ T. That ΔB is four times larger for the small structure than for the large structure suggests an AB-type interference effect. This is because the two-times difference in scale between the two structures makes a four-times difference in the window area. Actually, the area encircled by the sold line in Fig. 1(b) is approximately $S=0.9$ μm^2 for the large structure with $E_F=6$ meV, which agrees with $\Delta B=(h/eS)=4.6$ mT. The negative R_{L1}